IRIS AperTO

UNIVERSITÀ DEGLI STUDI DI TORINO

AperTO - Archivio Istituzionale Open Access dell'Università di Torino

Improved catalytic performance of hierarchical ZSM-5 synthesized by desilication with surfactants

This is the author's manuscript

Original Citation:

Availability:

This version is available http://hdl.handle.net/2318/123334 since 2016-10-03T19:55:44Z

Published version:

DOI:10.1016/j.micromeso.2012.07.045

Terms of use:

Open Access

Anyone can freely access the full text of works made available as "Open Access". Works made available under a Creative Commons license can be used according to the terms and conditions of said license. Use of all other works requires consent of the right holder (author or publisher) if not exempted from copyright protection by the applicable law.

(Article begins on next page)

25 April 2024

UNIVERSITÀ DEGLI STUDI DI TORINO

This Accepted Author Manuscript (AAM) is copyrighted and published by Elsevier. It is posted here by agreement between Elsevier and the University of Turin. Changes resulting from the publishing process - such as editing, corrections, structural formatting, and other quality control mechanisms - may not be reflected in this version of the text. The definitive version of the text was subsequently published in F. Schmidt, M. R. Lohe, B. Büchner, F. Giordanino, F. Bonino, S. Kaskel (2013) **Improved catalytic performance of hierarchical ZSM-5 synthesized by desilication with surfactants,** MICROPOROUS AND MESOPOROUS MATERIALS (ISSN:1387-1811), pp. 148- 157. Vol. 165.

You may download, copy and otherwise use the AAM for non-commercial purposes provided that your license is limited by the following restrictions:

(1) You may use this AAM for non-commercial purposes only under the terms of the CC-BY-NC-ND license.

(2) The integrity of the work and identification of the author, copyright owner, and publisher must be preserved in any copy.

(3) You must attribute this AAM in the following format: Creative Commons BY-NC-ND license (http://creativecommons.org/licenses/by-nc-nd/4.0/deed.en), http://dx.doi.org/10.1016/j.micromeso.2012.07.045

Improved catalytic performance of hierarchical ZSM-5 synthesized by desilication with surfactants

Franz Schmidt[a], Martin R. Lohe[a,b], Bernd Büchner[b], Filippo Giordanino[c], Francesca Bonino[c], Stefan Kaskel[a,d]

[a] Department of Inorganic Chemistry, Dresden University of Technology, Bergstr. 66, 01069 Dresden, Germany

[b] Leibniz Institute for Solid State and Materials Research Dresden (IFW Dresden), Institute for Solid State Research, Helmholtzstrasse 20, 01069 Dresden, Germany

[c] Department of Chemistry, NIS Centre of Excellence, and INSTM Centro di Riferimento, University of Turin, Via P. Giuria 7, I-10125 and Via Quarello 11, I-10135, Torino, Italy.

[d] Fraunhofer Institute for Material and Beam Technology IWS, Winterbergstr. 28, 01277 Dresden, Germany

Corresponding Author: Stefan Kaskel

Full Mailing Address:

Department of Inorganic Chemistry,

Dresden University of Technology,

Bergstrasse 66, D-01069 Dresden, Germany

Telephone: +49-351-46333632

Fax: +49-351-46337287

Email: stefan.kaskel@chemie.tu-dresden.de

Abstract

Hierarchical ZSM-5 zeolites were synthesized by alkaline desilication and a surfactant induced re-assembly. Contrary to the purely alkaline desilicated zeolites a strong increase in external surface area, a narrow pore size distribution of 3-10 nm and a decreased Brönsted acidity could be achieved when using CTAB as a surfactant throughout the alkaline treatment. The hierarchical pore system and the decreased acidity lead to an improved catalyst lifetime in the methanol to hydrocarbon conversion. A further improvement could be accomplished by increasing the surfactant concentration during the desilication re-assembly preparation. Tailoring of mesopore size and specific surface area was achieved using surfactants with different chain lengths.

1. Introduction

Zeolites are crystalline aluminosilicate materials with a well defined microporous structure and tunable intrinsic properties. These characteristic properties are very attractive for industrial processes, especially catalysis, separation and ion-exchange steps. In catalytic applications acidity and well defined pore sizes are deceisive, leading to a high selectivity in industrial processes. The ZSM-5 is an often used and well established industrial zeolite for catalytic processes such as the alkylation of benzene, the isomerization of m-xylene or the conversion of methanol to hydrocarbons [1-2]. Especially the MTH (methanol-to-hydrocarbon)-process recently gained a lot of attention due to the declining crude oil resources. However, the beneficial properties of the small definite pore openings cause diffusion limitations of larger reacting molecules, leading to restrictions in the catalyst activity and lifetime. To overcome this problem a lot of research has been done in the last years to shorten the diffusion length in zeolites, either by reducing the particle size [3-4] or by introducing an additional mesoporous transport network [5-8]. The introduction of such a network can be achieved by hard-templating [5, 9-10] or soft-templating [11-13] techniques. Another possibility is the desilication of high silica zeolites (especially ZSM-5) with alkaline solutions, established by Groen et al. [14-17]. This method is cost efficient and facile. The drawback of the desilication is the loss of zeolite material due to the leaching process and the relatively unselective mesopore formation. Furthermore the zeolite composition dictates the degree of desilication and therefore this technique is limited to chemical composition of Si/Al = 25-50. Recent process optimization expanded the range of effective mesopore formation to a Si/Al ratio of 12 – 200 [18-20]. These Si/Al desilication ranges are typical for ZSM-5 zeolites, but are not generally applicable to other zeolite topologies.

Another approach generating mesoporosity by dissolution involves the simultaneous re-assembly of amorphous silica directed by surfactant molecules. The literature describes several methods to transform silica spheres pseudmorphic to mesoporous M41S-type

materials [21-22]. The re-assembly of completely dissolved zeolitic structures around surfactant molecules was also reported [23-27]. In 2004 Ying et al. adapted the concept of pseudomorphic transformation for zeolitic systems [28]. Slightly alkaline and hydrothermal reaction conditions enabled the introduction of mesoporosity in zeolite FAU, MOR and MFI. Ying and García-Martínez proposed a surfactant-assisted crystal rearrangement mechanism [29, 30]. In 2012 Yoo et al. published a dissolution re-assembly process under different synthesis conditions [31] being close to the conditions described for pure desilication procedures. Dissolved fragments of ZSM-5 were reassembled around CTAB molecules and re-deposited on the zeolite surface. In parallel we developed a similar synthesis route, but without a hydrothermal treatment.

In the following we described the applicability of such a hierarchical material in the methanol to hydrocarbon catalysis. The effects of the surfactant concentration on the catalytic performance will be reported. Finally, tailoring the size of the introduced mesopores by changing the applied surfactant micelle molecules was successful.

2. Experimental

2.1. Catalyst preparation

2.1.1 Conventional ZSM-5

The synthesized ZSM-5 (Z50, Z100 and Z300) were prepared by a modified synthesis of Jacobs et al. [32]. A mixture containing 3.7 g SiO_2 (Aerosil 200), 0.839 g TPABr, 0.487 g NaOH and 33.6 g H_2O was prepared and stirred for 24 h. Later on a solution consisting of 0.101 g (in case of Z100: 0,051 g and Z300: 0.017 g) of $NaAlO_2$ and 6.4 g H_2O was added slowly to the silica containing mixture. For the Z50 a molar ratio of 100 SiO_2 : 2 Al : 5.1 TPABr : 3600 H_2O was obtained. The preparation of the Z300 material resulted in a molar ratio of: 100 SiO_2 : 0.34 Al : 5.1 TPABr : 3600 H_2O. The pH-value was adjusted to 11 with concentrated sulphuric acid. The mixture was placed in a teflon-lined stainless steel autoclave and treated hydrothermally at 423 K for 72 h. The obtained powder was washed several times with distilled water, dried for 5 h at 373 K and afterwards calcined in air for 5 h at 823 K. To obtain the H-form of the zeolite, the powder was treated three times with 20 $ml/g_{zeolite}$ of a 0.5 M NH_4NO_3 solution.

2.1.2 Alkaline treated ZSM-5

The alkaline treated ZSM-5 samples were denoted as –at (e.g. Z50-at). The desilication procedure was performed by treating the starting material (Na-ZSM-5) with 20 $ml/g_{zeolite}$ of a 0.5 M NaOH-solution. The mixture was stirred for 24 h at 353 K and afterwards cooled in an ice bath to stop the desilication. The obtained powder was washed three times and dried over night at 353 K. The acidic form was obtained as described above.

2.1.3 Alkaline reassembled ZSM-5

Recently Yoo at al. published a synthesis route which combines desilication and re-assembly of zeolites using N,N,N-Trimethylhexadecylammoniumbromid (CTAB) as a micelle forming

molecule [31]. The synthesis used in this work is slightly different. Basically the synthesis conditions are identical to those of the alkaline treated ZSM-5, despite that the sodium hydroxide solutions contains a certain amount of the surfactant. In the standard procedure the concentration of CTAB was 0.05 M. In further experiments the amount and the chain length of the surfactant was varied.

For clarification the catalyst preparation is summarized in Table 1.

Table 1: Summary of the desilication treatments applied; Z50, Z300, Z140 stands for a ZSM-5 with a theoretical Si/Al ratio of 50; 300 and 140 respectively; -at corresponds to 'alkaline treated'; -com is the abbreviation for commercial

sample code	desilication treatment	
	c(NaOH) [mol l^{-1}]	c(CTAB) [mol l^{-1}]
Z50	-	-
Z50-at	0.5	-
Z50-at_0.05CTAB	0.5	0.05
Z50-at_0.1CTAB	0.5	0.1
Z50-at_0.2CTAB	0.5	0.2
Z300	-	-
Z300-at	0.5	-
Z300-at_0.05CTAB	0.5	0.05
Z140-com	-	-
Z140-com-at_0.05CTAB	0.5	0.05

2.2. Characterization of the ZSM-5 zeolites

X-ray powder diffraction patterns were obtained with a Panalytical XPert Pro diffractometer in reflection mode using a Ge-monochromated Cu $K\alpha_1$ radiation.

Nitrogen physisorption isotherms were conducted using a Quantachrome Autosorb 1C apparatus at 77 K. Prior to all measurements the samples were degassed under vacuum and 423 K for at least 24 h. The surface area was determined by applying the BET equation in the linear range (p/p_o = 0.01 – 0.15). The t-plot was used to evaluate the external surface area and

the micropore volume. The mesoporous volume was derived by subtracting the micropore volume from the overall pore volume ($p/p_0 = 0.98$).

SEM (Scanning Electron Microscope) was used to determine the size and the morphology of the zeolite particles. The measurements were performed with a DSM-982 Gemini (Zeiss) operating at 10 kV. Prior to the measurement the samples were prepared on a carbon pad and sputtered with gold to obtain the necessary conductivity. SEM photographs with a high magnification were used to visualize the formed mesopores.

For TEM investigation the samples were all prepared by ultrasonically assisted suspending in ethanol or isopropanol. The resulting suspension was dropped onto a copper grid coated with holey carbon and dried using an infrared lamp. The TEM investigations were carried out on a Cs-corrected JEOL JEM-2010F at an acceleration voltage of 80 kV.

Temperature programmed desorption of ammonia was performed with a BELCAT B (BEL Japan, Inc.). Approximately 80 mg catalyst was activated for one hour at 773 K heating with a ramp of 3 K/min. After cooling to 473 K pure ammonia (99.98 %) was passed over the sample. To remove the physisorbed ammonia the sample was purged with helium (99.999 %) with a flow of 20 mL/min for 5 h. Desorption of the chemisorbed ammonia was accomplished by heating until a temperature of 973 K.

The temperature-programmed decomposition (DTA/TG) of the surfactant molecule was carried out using a Netzsch STA 409 instrument. 20 mg of each sample were heated in a 100 ml/min air-stream at a rate of 5 K/min until 1270 K, while the mass change due to template decomposing was recorded.

FTIR measurements to characterize the hydroxy groups in zeolite materials were performed on a Nicolet 6700 FTIR spectrometer, operating in transmission mode at 2 cm^{-1} resolution on self-supported pellets. The samples were pretreated at 773 K at $p << 1 \times 10^{-4}$ mbar for 2 h, heating them from room temperature to 773 K with 3 K/min. On the treated samples the OH groups were further characterized with CO probe molecule at low temperature (T = 77 K).

The differences in acid strength and distribution of the different OH groups were derived from the changes in IR absorption of CO probe molecules adsorbed at 77 K and a partial pressure of 70 mbar.

2.4. Catalytic tests

All catalytic tests were performed in a quartz glass fixed bed reactor (i.d. 11 mm). 1 g of crushed and sieved (125 µm – 315 µm) zeolitic catalyst was mixed (to avoid inhomogeneous flow) with 4 g of inert porous silica gel (d = 60-200 µm), resulting in a dumping height of 8 cm. The catalyst bed was activated in a pure helium flow (26 L/h) at 773 K for 90 min prior each run. Then the temperature was set to 673 K and the helium flow was mixed via a CEM (controlled evaporator mixer) with 4 g/h methanol, resulting in a weight hourly space velocity (WHSV) of 4 gram methanol per gram catalyst per hour (g g^{-1} h^{-1}). All experiments were carried out under atmospheric pressure and a methanol partial pressure of p_{MeOH} = 0.1 bar. Product analysis was performed using gas chromatography. The effluent composition was determined with an on-line Perkin Elmer Clarus 500 FID equipped with an Elite SB5 column (60 m x 0.32 mm x 1 µm). For the selectivity analysis (after 20 min), the gas chromatograph was programmed with the following temperature program: 223 K for 6 min and heating with 10 K/min to 483 K. Helium was used as a carrier gas and after 5 min the column pressure was increased from 100 kPa to 200 kPa with 100 kPa/min. For the determination of the methanol conversion the same temperature program, just starting at 308 K, was used.

3. Results

3.1. Comparison of alkaline and alkaline surfactant treated zeolite

The desilication re-assembly and the classical desilication technique were compared with regard to their physiochemical and catalytic properties. Several zeolites with different composition and morphology were chosen to demonstrate that the concept of desilication and re-assembly is not limited by these parameters. A detailed characterization was performed with the synthesized ZSM-5 (Si/Al = 50). Fig. 1 shows the nitrogen physisorption isotherms and the derived pore size distributions of the parent (Z50), the alkaline treated (Z50-at) and the CTAB alkaline treated zeolite (Z50-at_0.05CTAB). The Z50 material has a typical type I isotherm, with a high nitrogen uptake at relatively low pressures. The isotherm is characteristic for purely microporous materials. The alkaline treated material (Z50-at) shows a strong increase in nitrogen adsorption at pressures higher than $p/p_0 = 0.4$. The pore size calculated with the BJH-equation from the desorption branch shows a broad size distribution ranging from 10 – 100 nm. The isotherm of the alkaline surfactant treated ZSM-5 (Z50-at_0.05CTAB) is a combination of a type I and type IV isotherm typical for hierarchical materials. The uptake of nitrogen could be increased significantly in the low pressure region as well as at pressures above $p/p_0 = 0.4$. In contrast to the purely alkaline treated material, the surfactant assisted templating results in a material, with very narrow mesopore size distribution ranging from 3 – 10 nm.

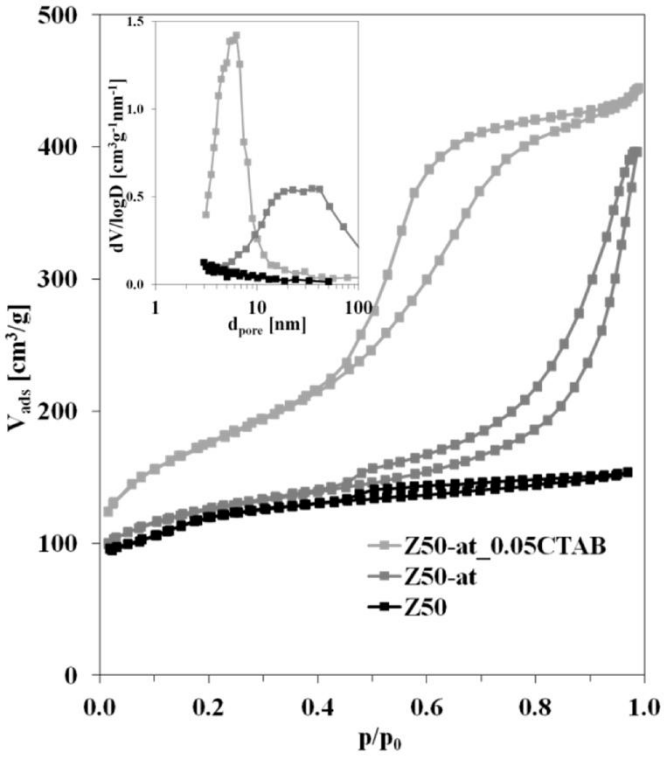

Figure 1: Nitrogen physisorption isotherms for the untreated zeolite (Z50), the desilicated zeolite (Z50-at) and the desilicated reassembled zeolite (Z50-at_0.05CTAB). The inset displays the BJH pore size distribution derived from the desorption branch.

The adsorption data are summarized in Table 2. The alkaline re-assembly technique was applied for different ZSM-5 systems as well. The Z300 sample is a ZSM-5 with a theoretical Si/Al ratio of 300. Furthermore a commercial zeolite with a composition of Si/Al = 140 was investigated. The total BET surface areas increased about 250 m^2/g for all three samples after treating the starting material with sodium hydroxide and CTAB. The high BET surface area is ascribed to an increased mesoporous surface area, whereas the microporous amount decreases. Mesopore surface areas up to 536 m^2/g could be generated using this method. The obtained isotherms have almost an identical shape (supplementary information Fig. S1), indicating that the generated mesoporosity is independent from the zeolitic framework composition and morphology. The alkaline treatment has also a considerable impact on the pore volume. The total pore volume was calculated from the adsorbed amount of nitrogen at

p/p_0 = 0.98. As reported in the literature the desilication with sodium hydroxide leads to a significant increase in total pore volume and to a decrease in microporevolume [19]. However, this effect is more pronounced for zeolites with a chemical composition of Si/Al = 25-50. The classic desilication technique is not suitable for ZSM-5 zeolites with high silicon to aluminum ratios [14]. Using CTAB as a surfactant during the alkaline treatment the same results could be obtained independently from the framework composition.

With regard to the chemical composition it is obvious that due to almost selective silicon extraction the alkaline treated zeolites have a decreased Si/Al ratio. However, the silicon extraction is reduced when using CTAB additionally. A reason for this reduction is presumably the CTAB induced re-assembly of the dissolved silicon rich zeolite fragments around the remaining zeolite particle. The observations are in good agreement with the reduced desilication loss when using additional surfactants.

The combination of an increased mesopore surface area and a decreased desilication loss subsequently leads to a higher desilication efficiency. The desilication efficiency has been introduced by Verboekend et al. [33] to quantify the degree of dissolution with the introduced mesoporosity. Where the purely alkaline treated zeolites showed desilication efficiencies of 2 m^2g^{-1} per percent zeolite loss or worse, the zeolites with the additional use of CTAB had efficiencies of around 7 - 8 m^2g^{-1}.

Table 2: Textural characteristics of parent and hierarchical ZSM-5 materials

	S_{BET}		V_{Pore}		Si/Al [d]	Yield [e]	Desilication efficiency
	total [a]	S_{meso} [b]	total [c]	V_{micro} [b]			
	$[m^2 g^{-1}]$	$[m^2 g^{-1}]$	$[cm^3 g^{-1}]$	$[cm^3 g^{-1}]$	$[mol\ mol^{-1}]$	[%]	$[m^2 g^{-1}]\%^{-1}$
Z50	417	55	0.237	0.152	51	-	-
Z50-at	455	229	0.693	0.095	14	21	2.2
Z50-at_0.05CTAB	626	439	0.687	0.079	25	50	7.6
Z300	393	81	0.211	0.119	289	-	-
Z300-at	385	105	0.311	0.108	14	20	0.3
Z300-at_0.05CTAB	663	520	0.700	0.062	119	37	7.0
Z140-com	379	99	0.210	0.108	142	-	-
Z140-com-at_0.05CTAB	645	536	0.785	0.048	63	42	7.5

[a] S_{BET} was calculated by applying the multi-point BET equation in the linear range.

[b] S_{meso} and V_{micro} were calculated by applying the t-plot-method.

[c] V_{pore} was calculated from the adsorption branch at ($p/p_0 = 0.98$).

[d] The elemental composition was determined by ICP-OES.

[e] The desilication yield was determined by weight measurement of the treated samples after calcination.

Fig. 2 shows the X-ray diffraction pattern of a zeolite treated with sodium hydroxide and additional CTAB in comparison to the parent material. The crystallinity is well preserved for both alkaline treated samples, even though the (101) peak of the alkaline treated zeolite is slightly reduced. No reflections were observed in the low angle 2θ-region, indicating that the obtained mesopores for both alkaline treated samples are not ordered.

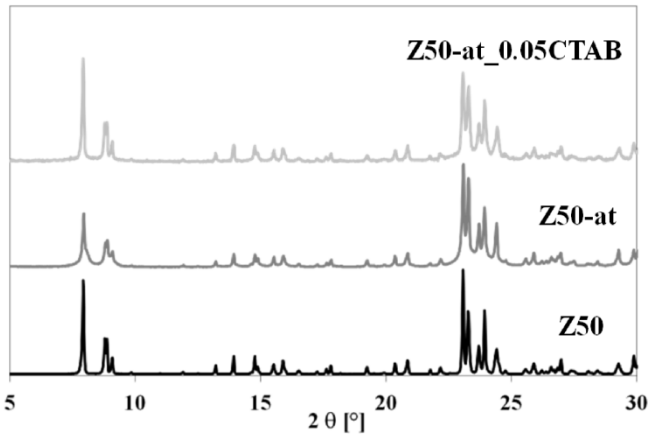

Figure 2: XRD pattern of the untreated (Z50), the desilicated (Z50-at) and the desilicated reassembled (Z50-at_0.05CTAB) samples.

SEM pictures (Fig. 3) of the ZSM-5 zeolites, exemplarily for the Z50 samples, revealed that the typical ZSM-5 morphology is maintained throughout the alkaline treatment. The surface of the parent ZSM-5 zeolite is already quite rough, which is typical for high aluminum contents (Fig. 3a,b). The surface nature of the sodium hydroxide treated crystals is somehow ruggedly and shows voids (Fig. 3c,d). This surface abrasiveness corresponds to the results obtained from the nitrogen physisorption measurements, revealing pore sizes of 10 - 100 nm were observed. When CTAB is used throughout the desilication the surface is more smoothened, although the characteristic surface properties of the parent ZSM-5 disappeared (Fig. 3e,f). The morphology of the other zeolite samples with higher Si/Al ratio is preserved as well (supplementary information Fig. S2).

TEM images of the desilicated reassembled zeolite (Z50-at_0.05CTAB) revealed the presence of the mesopores (Fig. 3g) and also indicated that there is no ordering of these pores. Fig 3h clearly shows the micropores of the ZSM-5 at the surface of the ZSM-5 particle. It is also visible that the pores (straight channels in [010]) are not oriented in one direction, which is an indication, that zeolitic parts have been reassembled on the surface of the remaining zeolite particle.

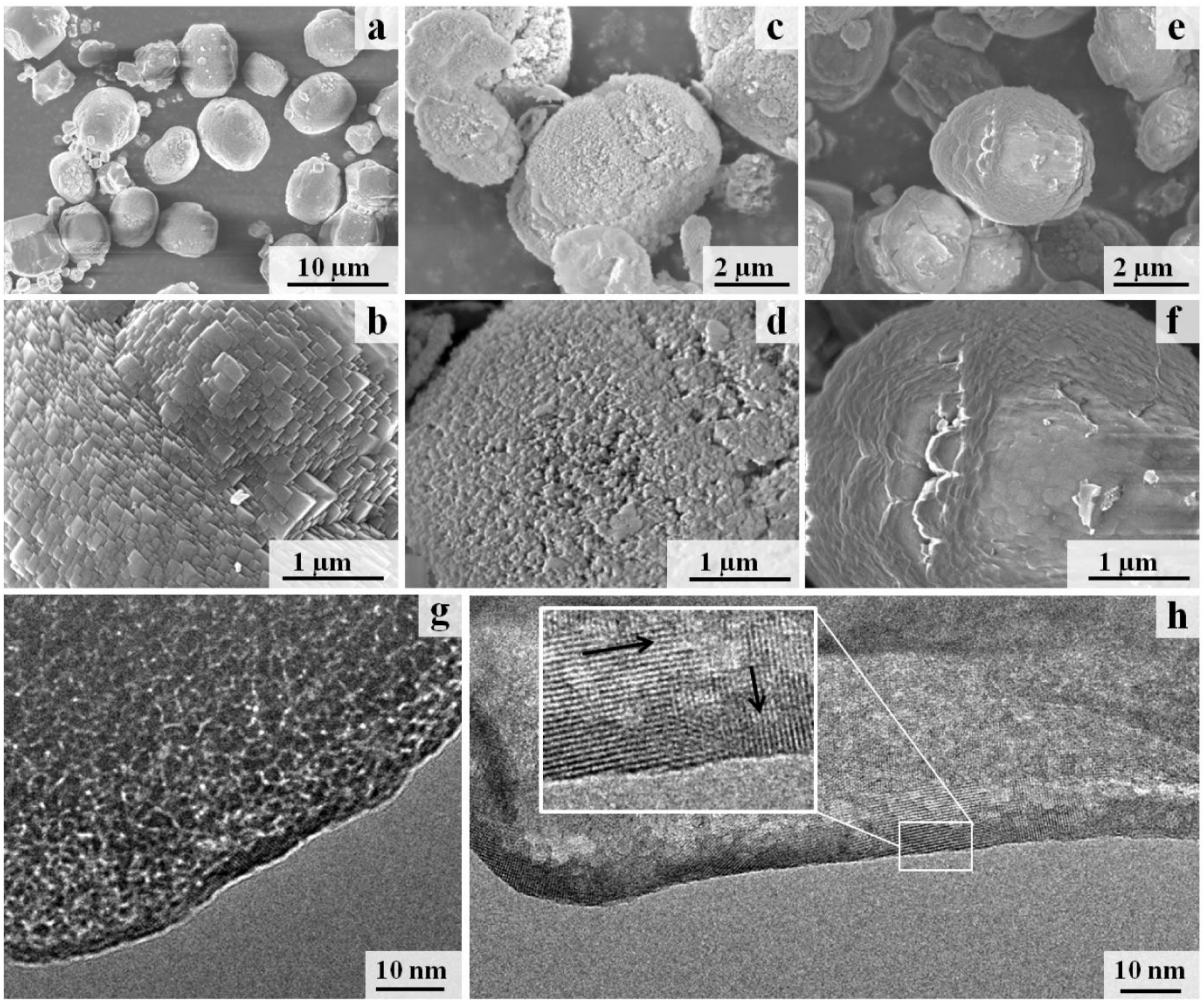

Figure 3: SEM images of a) and b) parent ZSM-5 (Z50); c) and d) desilicated ZSM-5 (Z50-at); e) and f) desilicated reassembled ZSM-5 (Z50-at_0.05CTAB). TEM images g) and h) of the desilicated re-assembled ZSM-5 (Z59-at_0.05CTAB).

FTIR measurements with pulsed CO adsorption were performed to compare the acidic properties of the samples (Fig. 4). The spectra in the left column show the hydroxyl group range (3800 – 3000 cm^{-1}) while those ones in the right column report the CO-vibrational modes (2250 – 2060 cm^{-1}) range. The bold black curves show background spectra (*i.e.* outgassed sample), the bold grey curves refer to highest CO coverage, while the slim gray curves report intermediate adsorption steps. In order to allow band intensity comparison within the full set of spectra, a normalization to the overtone modes in the 1750–2100 cm^{-1} region has been performed.

The existence of different types of acid sites for the untreated zeolite is revealed. At low CO coverage, the first band developing is from Brönsted acid sites at 3614 cm^{-1} which is shifted to 3278 cm^{-1} indicating that the Brönsted acid sites are the most acidic sites in the zeolite. Upon increasing the CO pressure, the band a 3734 cm^{-1} shifts to 3651 cm^{-1}. This change is assigned to CO interacting with the silanols. The CO stretching region shows that at very low coverage, a band located at 2173 cm^{-1} is observed, corresponding to CO interacting with Brönsted sites. At a higher coverage, an asymmetric band centered at 2156 cm^{-1} is observed, which is assigned to CO interacting with the silanols. The sharp band at 2137 cm^{-1} refers to a liquid-like phase condensed into the pores of the zeolite.

Z50 and Z50-at have a comparable Brönsted acidity although slightly reduced in the case of Z50-at sample. An increase of the silanol stretching mode at 3750 cm^{-1} for the alkaline treated sample is in well accordance to the increased external surface area of this material. On the other hand the CTAB alkaline treated sample showed only a small signal at 3617 cm^{-1} and a reduced signal in the CO region indicating a low Brönsted acidity. The amount of isolated silanols is strongly increased in comparison to the other two samples. Additionally, the CTAB alkaline treated sample shows clearly Brönsted species linked to partially extraframework Al (band at 3672 cm^{-1}) and obviously perturbed upon CO adsorption and a small amount of Lewis acidity (small contribution at 2230 cm^{-1} in the CO region). However, the literature reports a diminished extinction coefficient for Lewis acid sites, which makes them hard to compare with the Brönsted acid sites [34].

The acid site density was determined by ammonia desorption measurements (supplementary information Fig. S3; Tab. S1). The desorption peak around 500 – 800 K was deconvoluted into two peaks, one centered around 700 K and one around 600 K. For evaluation of the acid site density only the 700 K peaks were compared, since it is reported that these sites are active in the MTH catalysis [35]. The desorption profiles for both desilicated samples show a distinctive shoulder at 550 – 650 K, indicating the presence of different acid sites (most likely

Lewis acid sites). Aluminate species remaining in the zeolite after the desilication are responsible for this shoulder in the TPAD profile. The surfactant treated material shows a distinctive reduction in strong acid sites, which is in agreement with the reduction of Brönsted acid sites observed in the CO-FTIR measurements.

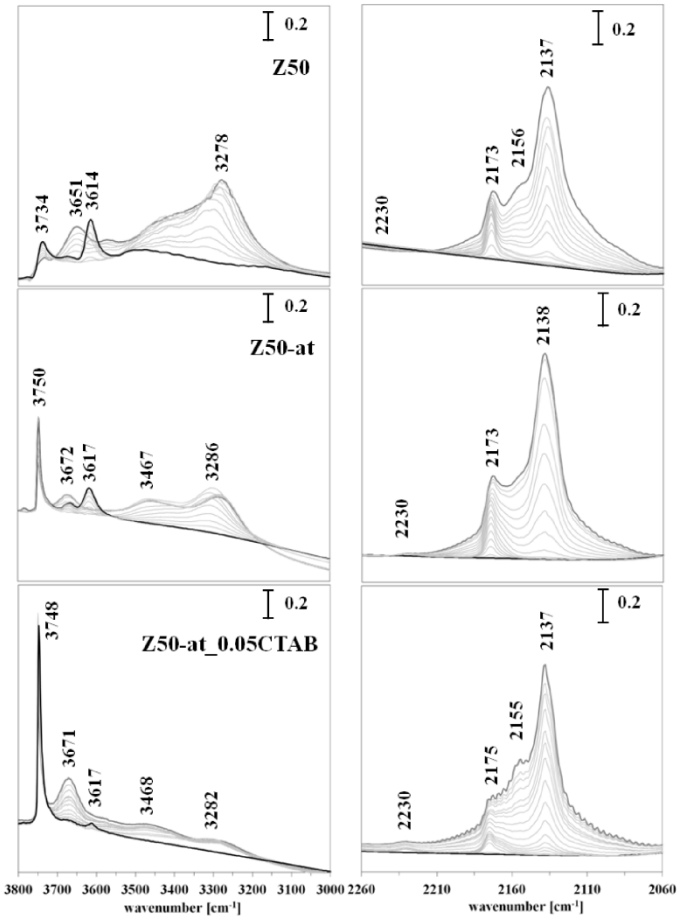

Figure 4: FTIR spectra of parent (Z50), the desilicated (Z50-at) and the desilicated reassembled (Z50-at_0.05CTAB) material before and after pulsed CO adsorption. Shown are the OH vibrational modes (left) and the CO vibrational modes (right).

Fig. 5 displays the catalytic lifetime of the parent and the different alkaline treated samples (Z50 charge). All three zeolites show a complete conversion of methanol and dimethylether for at least 20 h. After this time the conversion of the untreated zeolite (Z50) decreases. After 40 h time on stream the hydrocarbon yield drops below 50 % of conversion. The alkaline

treated zeolites has a longer catalyst lifetime with a decrease of hydrocarbon yield after 55 h. However, the deactivation rate of the alkaline surfactant treated zeolite is clearly slower than that of the purely alkaline treated one. The 50 % conversion mark of the alkaline surfactant treated sample is reached after about 90 h time on stream. To distinguish between the effect of acidity and mesoporosity on the catalytic performance, the lifetime of the Z100 catalyst is shown as well (dashed line). This catalyst is comparable with the alkaline surfactant treated zeolite referring to acidity and crystal size (supplementary data Tab. S1) but differs in terms of additional porosity (supplementary data Fig. S4). The Z100 zeolite shows a better catalytic performance than the Z50 zeolite, which is ascribed to the reduced acid site density. However, the positive effect of additional porosity becomes visible, when comparing the Z100 zeolite with the alkaline surfactant treated zeolite (Z50-at_0.05CTAB).

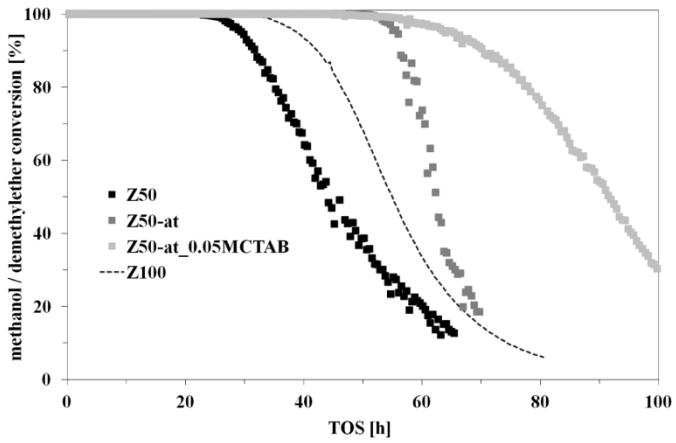

Figure 5: Catalytic lifetime in the conversion of methanol of the parent (Z50), the desilicated (Z50-at) and the desilicated reassembled (Z50-at_0.05MCTAB) material. The dashed line (Z100) corresponds to a purely microporous zeolite with comparable acidic properties as the desilicated reassembled zeolite

Fig. 6 shows the product distribution of the three catalysts. It is obvious that the desilication has a crucial impact on the different hydrocarbon fractions. The C_3 (predominantly propene) selectivity is approximately 27 % and the highest for the Z50 zeolite (Fig. 6a). Whereas the pure alkaline treated zeolite (Fig. 6b) shows the lowest selectivity for C_3 molecules (around

20 %). For all three catalysts it is clearly visible that shortly before the deactiviation the amount of C_3 molecules strongly increases. The highest amount of C_6^+ hydrocarbons (around two thirds are aromatic molecules) is observed for the alkaline treated zeolite. The amount of C_6^+ molecules decreases for all three catalysts with time on stream. An explanation for these results could be the restricted molecular diffusion upon increasing coke deposition [36]. The amount of C_4 alkanes (C_4^-) correlates in some way with the C_6^+ hydrocarbons since alkanes and hydrocarbons entail each other via hydride shift reactions.

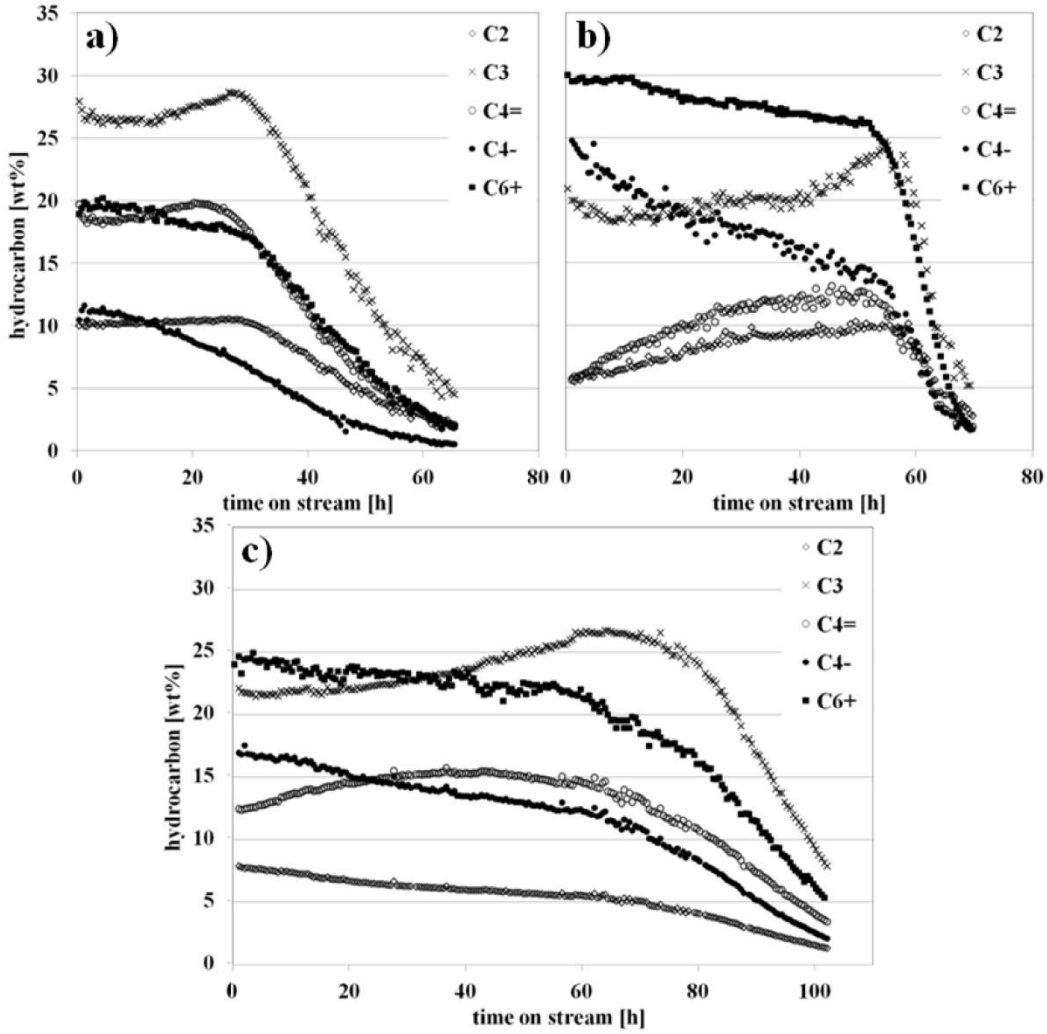

Figure 6: The product distribution vs time on stream in the MTH reaction of a) the parent (Z50), b) the desilicated (Z50-at) and c) the desilicated reassembled (Z50-at_0.05CTAB) material.

3.2. Variation of the surfactant concentration

Since the use of the co-additive CTAB leads to an improved performance in the conversion of methanol, the concentration of this surfactant was varied during the desilication procedure. The concentration of CTAB was increased to 0.1 M and 0.2 M (denoted as _0.1CTAB and _0.2CTAB respectively). The intent of this experiment was to enhance the external surface area and pore volume even further. If the external surface area increases, it is likely that the catalytic lifetime of the material increases as well [37]. All materials showed a well preserved MFI phase crystallinity, but no peaks in the small angle range were observed, indicating that no ordered mesoporous phase was obtained. The nitrogen physisorption isotherms of the desilicated reassembled materials are shown in Fig. 7a. The shapes of the isotherms are similar, although the materials treated with higher CTAB concentrations have an increased meso-/macropore volume (Tab. 3). The chemical composition of the resulting product is not affected by varying the surfactant concentration.

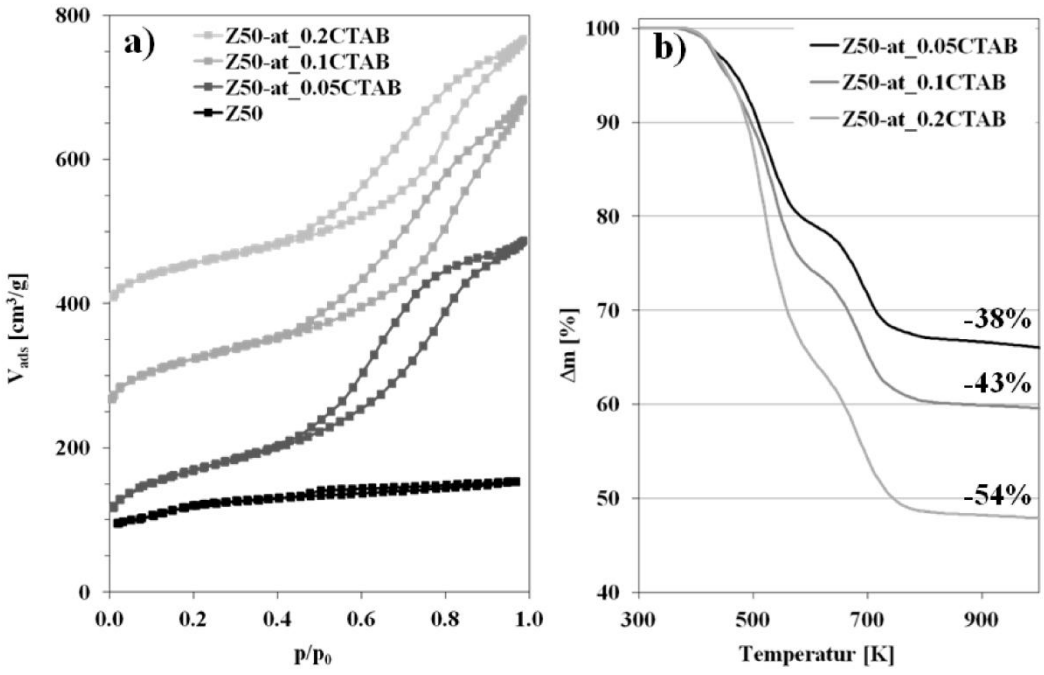

Figure 7: a) Nitrogen physisorption isotherms (offset: Z50-at_0.1CTAB = 150 cm^3/g; Z50-at_0.2CTAB = 300 cm^3/g) of desilicated reassembled samples using different concentrations of CTAB. b) Thermogravimetric data of the samples using different surfactant concentrations during combustion in air.

Table 3: Textural characteristics of parent and hierarchical ZSM-5 materials synthesized using different concentration of CTAB.

	S_{BET}		V_{Pore}		Si/Al [d]	Yield [e]	Desilication efficiency
	total [a]	S_{meso} [b]	total [c]	V_{micro} [b]			
	$[m^2 g^{-1}]$	$[m^2 g^{-1}]$	$[cm^3 g^{-1}]$	$[cm^3 g^{-1}]$	$[mol\ mol^{-1}]$	[%]	$[m^2 g^{-1}]\%^{-1}$
Z50	417	55	0.237	0.152	51	-	-
Z50-at	455	229	0.693	0.095	14	21	2.2
Z50-at_0.05MCTAB	626	439	0.687	0.095	25	50	7.6
Z50-at_0.1MCTAB	578	357	0.734	0.093	26	59	7.2
Z50-at_0.2MCTAB	635	436	0.794	0.084	24	50	7.6

[a] S_{BET} was calculated by applying the multi-point BET equation in the linear range.

[b] S_{meso} and V_{micro} was calculated by applying the t-plot-method.

[c] V_{pore} was calculated from the adsorption branch at ($p/p_0 = 0.98$).

[d] The elemental composition was calculated by ICP-OES.

[e] The desilication yield was calculated by weight measurement of the treated samples after calcinations.

Fig. 7b shows the thermogravimetric data of the CTAB templated samples heated in air. A clear trend is observable, that with an increased amount of CTAB during the desilication, more CTAB is incorporated in the hierarchical material. The thermogravimetric data is in accordance with the total pore volume derived from the nitrogen physisorption data. All three samples show a two step mass loss, one at 420 – 590 K and one at 600 - 800 K. The literature describes this by a stepwise degradation of the CTAB template.

The obtained materials were catalytically tested. Fig. 8 displays the conversion capacity of each catalyst until a 50 % hydrocarbon yield. The black bars express the amount of converted methanol per gram zeolite. The grey bars represent the relative amount, when the loss due to the desilication procedure is taken into account. The disadvantage of the alkaline desilication is, that the improved catalytic performance is compensated by the high loss of zeolite material. In case of using CTAB as a surfactant the catalytic performance outperforms the

parent material even when taking the loss into account. It is clearly visible that not only the amount of external surface area is responsible for the conversion capacity, but also the pore volume, which can be tailored by the amount of incorporated surfactant.

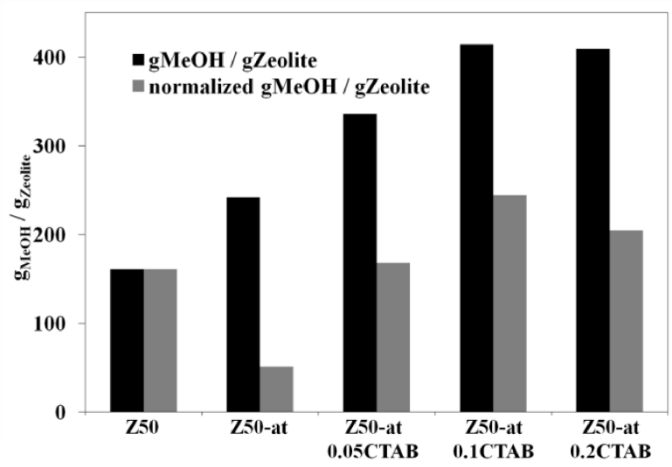

Figure 8: Conversion capacity of the samples synthesized with different surfactant concentration. The amount of converted methanol was calculated until the hydrocarbon yield dropped below 50 %.

3.3. Variation of the surfactant chain length

CTAB was used as the co-additive in the previous experiments. If the surfactant molecule is responsible for the mesopore formation, it was investigated if the pore size of these mesopores is tunable by varying the chain length of the surfactant molecule. Instead of using hexadecyltrimethylammonium bromide (C16) as the surfactant other molecules like tetradecyltrimethylammonium bromide (C14), dodecyltrimethylammonium bromide (C12), decyltrimethylammonium bromide (C10) and octadecyltrimethylammonium bromide (C18) were used during the alkaline treatment.

As a result of the nitrogen physisorption measurements a linear correlation between the specific BET surface area and the alkyl chain length of the applied surfactant was observed (Fig. 9a).

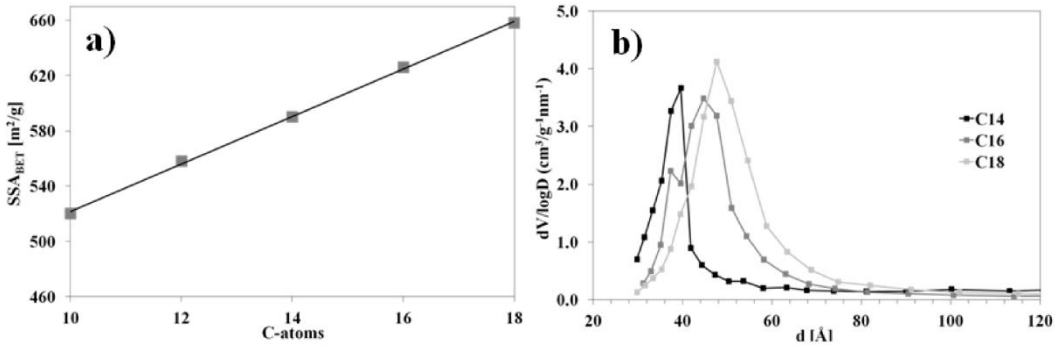

Figure 9: Data derived from the nitrogen physisorption measurements for the samples templated with different surfactant molecules. a) correlation of BET surface area and template chain length; b) mesopore size distribution

The corresponding nitrogen physisorption isotherms (supplementary information Fig. S5) show that with increasing chain length a more distinctive H2 hysteresis type is pronounced. To describe the pore size distribution the BJH model derived from the desorption branch was applied. Due to the tensile strength effect the model was only applied for the surfactants with 14, 16 and 18 c-atoms chain length to obtain valuable data. It is clearly visible that the chain length determines the mesopore size distribution. Although there are some indications that the pore size distribution of the C16 and especially the C14 is influenced by the tensile strength effect, the desorption model was applied since it gives the most accurate description of the pore sizes in this region. The pore size distribution derived from the adsorption branch shows the same trends, but with an overestimation of the actual mesopore size. However, the correlation between mesopore size and surfactant chain length was only observable for the sodium form. After the exchange with an ammonium nitrate solution the mesopores become widened and the defined differences in the distribution are lost (supplementary information Fig. S6).

4. Discussion

4.1. Comparison alkaline and alkaline template treated zeolite

Several zeolites with different composition were compared by desilication in purely alkaline media and alkaline media with additional surfactant molecules. The nitrogen physisorption data shows, that with the use of CTAB as a soft-template the amount of external surface area can be remarkably increased up to 536 m^2/g. To our knowledge this is the highest value which has been obtained by desilication treatment of ZSM-5 [20]. The purely alkaline treated zeolite samples showed increased external surface areas as well, but not in the extent as the surfactant treated samples. The literature reports that the zeolite composition has a crucial impact on the formation of mesoporosity in zeolites [14, 19]. Aluminum has a directing influence on the desilication and a ZSM-5 composition of Si/Al = 25-50 was found to be optimal. Similar results were obtained in this work. Interestingly the chemical composition had no significant impact on the mesopore formation when CTAB was used as a surfactant during the alkaline treatment. The shapes of the nitrogen physisorption isotherms (supplementary information Fig. S1) were almost identical and the obtained values for external surface area and pore volume were in the same range. On the other hand SEM studies revealed that no additional mesoporous phase was formed. The literature ascribes this increased external surface area to the dissolution and re-assembly of extended zeolite fragments [30, 31]. The dismantled negatively charged zeolite species interact with the positively charged surfactant molecules (charge matching). The surfactant molecules self-assemble to micelles due to the interaction of the hydrophobic tail with the aqueous solution. The micelles redeposit on the zeolite surface and after combustion and calcination the zeolitic mesopore remains. Support for this hypothesis comes from the BJH analysis, which shows a quite narrow pore size distribution around $3 - 10$ nm. In comparison the purely alkaline treated materials have pore size distributions from $10 - 100$ nm; similar values were reported in the literature [14-15]. A

further evidence for this redeposition of extended zeolite fragments on the surface of the zeolite is the increased yield, while using CTAB during the desilication.

TEM pictures show that the reassembled material is not just mesoporous silica material. In fact zeolitic fragments are clearly visible at the outer part of the particle. SAXS studies revealed the mesopores are not ordered on a long range. However, no clear statement could be found on the shape and the orientation of the mesopores. Presumably the CTAB molecules form spherical micelles with zeolitic fragments around.

H-ZSM-5 is an important catalyst in the conversion of methanol to hydrocarbons, with high selectivity towards propene and excellent activity as well as longevity. A high Si/Al is preferred due to the reduced deactivation and high selectivity towards short chain olefins at low acid site densities. The increased acid site density of the desilicated ZSM-5 therefore explains the low amount of propene and the high yields of aromatic and aliphatic byproducts.

Dahl et al. suggested entrapped hydrocarbon species, in particular polymethyl benzenes, as reactive centers in the methanol conversion [38,39]. Several authors confirmed this hypothesis by isotopic switch experiments and nowadays the 'hydrocarbon pool mechanism' is the widely accepted mechanism for the MTH reaction [40-42]. Since the catalytic centers are inside the micropores of the zeolite, the correlation between mesopores and catalytic longevity is still under debate in the literature. Several papers have been published, reporting enhanced catalytic lifetime in hierarchically porous structures [37,43]. This phenomenon is attributed to an improved molecular diffusion through the mesopores. However, it has been proven that the deactivation of the ZSM-5 zeolite mainly occurs at the external surface due to coke formation [40]. Therefore an increased external surface area provides more potential reaction centers and the catalyst longevity increases [37,44]. In case of the CTAB treated materials the additional porosity is not the only reason for the improved catalytic lifetime. FTIR-measurements and NH_3-TPD revealed that the surfactant treated samples show a decrease in strong acid sites. To evaluate the influence of decreased acid site density and

additional porosity a purely microporous zeolite with comparable acidic properties was tested as well. The reduction of acid site density leads to an improved catalyst lifetime, which has been reported several times in the literature [44]. Therefore, the difference in catalyst lifetime of the Z100 and the Z50-at_0.05CTAB zeolite can be subscribed to the hierarchical pore system.

However, the superior catalytic performance is an interplay of acid site reduction and improved accessibility of these sites.

For clarification of the nature and density of the acid sites in the mesopores further experiments have to be performed. Additionally, a more size sensitive catalytic reaction could give further insight in the performance of these definite mesopores.

4.2. Variation of the surfactant concentration

By changing the surfactant concentration during the desilication re-assembly process it was possible to tailor the total pore volume of the final product, but no clear trend for the external surface area was observable. Applying a higher surfactant concentration resulted in a higher degree of incorporation for the CTAB molecules into the hierarchical zeolite, which subsequently lead to a higher pore volume after combustion. The pore size distribution or the chemical composition was not affected by the surfactant concentration. A higher surfactant concentration did also not result in the formation of an ordered mesoporous phase.

The catalytic test showed that the amount of converted methanol increased with higher surfactant concentration in the synthesis, meaning that the catalyst lifetime does not only depend on a high external surface area, as reported in earlier publications [37], but also on the total pore volume to some extent.

4.3. Variation of the surfactant chain length

The variation of the surfactant was carried out by changing only the longest alkyl chain of the alkyltrimethylammonium bromide. It is known from the literature that the size and phase of mesopores induced by the micelle formation is tunable by the alkyl chain length [45], but it is unknown in which extent this principle is adoptable to desilication re-assembly.

Small angle X-ray diffraction measurements did not show formation of a regular mesoporous phase, at the applied reaction temperature and the low surfactant concentration. Therefore the focus was not set on phase transformation, but on the changes of the mesopore size distribution. With increasing chain length, the diameter of the mesopores in the final product increased. This is a consequence of the micelle formation and described in the literature [45]. The results strengthen the proposed mechanism of micelle induced redeposition of zeolite fragments. Interestingly there is a linearly correlation between the BET surface area and the surfactant chain length. This observation could be attributed to an increased amount of combustible carbon introduced with larger chain length, resulting in a higher content of mesopores. However, these phenomena have only been observed for the Na-ZSM-5 form. Unfortunately the small definite pore size difference disappeared after the cation exchange. A deeper insight in this topic and a study concerning the influence of different mesopore sizes on catalysis will be performed in further experiments.

5. Conclusion

The desilication using CTAB as a co-surfactant of several ZSM-5 samples was performed. The obtained materials have beneficial properties in terms of surface area and pore volume, regardless of the chemical composition of the starting material. High external surface areas up to 536 m^2/g and narrow pore size distributions in the range of 3 – 10 nm were achieved by applying this method. The zeolitic structure and morphology of the treated materials have not been destroyed upon the desilication re-assembly process, although the acidic properties were conducive modified. Purely alkaline desilication of zeolites only lead to external surface areas of around 100 - 230 m^2/g, broad pore size distributions and an increased acid site density. Furthermore this technique destroys the starting material to some extent and is influenced by its chemical composition. By using a co-surfactant during the alkaline treatment, a hierarchical catalyst with high porosity and low acid site density was obtained.

The catalytic conversion of methanol to hydrocarbons confirmed the beneficial properties received by the physiochemical characterization. A further improvement in catalyst lifetime was achieved by introducing more surfactant molecules, leading to an increased catalyst porosity.

The size of the mesopores could be tailored by varying the longest alkyl chain of the tetra alkyl ammonium surfactant. However, the definite difference in pore size could not be retained upon ion exchange with NH_4NO_3.

Acknowledgments

We would gratefully acknowledge the Max-Buchner-Forschungsstiftung for a research scholarship and financial support.

Literature

[1] C.D. Chang, A.J. Silvestri, J. Catal, 47 (1977) 249-259.

[2] M. Stöcker, Microporous and Mesoporous Mater., 29 (1999) 3-48.

[3] I. Schmidt, C. Madsen, C.J.H. Jacobsen, Inorg. Chem., 39 (2000) 2279-2283.

[4] E. Biemmi, T. Bein, Langmuir, 24 (2008) 11196-11202.

[5] C.J.H. Jacobsen, C. Madsen, J. Houzvicka, I. Schmidt, A. Carlsson, J. Am. Chem. Soc., 122 (2000) 7116-7117.

[6] K. Egeblad, C.H. Christensen, M. Kustova, C.H. Christensen, Chem. Materials, 20 (2008) 946-960.

[7] J. Perez-Ramirez, C.H. Christensen, K. Egeblad, C.H. Christensen, J.C. Groen, Chem. Soc. Rev., 37 (2008) 2530-2542.

[8] M. Choi, K. Na, J. Kim, Y. Sakamoto, O. Terasaki, R. Ryoo, Nature, 461 (2009) 246-249.

[9] I. Schmidt, A. Boisen, E. Gustavsson, K. Stahl, S. Pehrson, S. Dahl, A. Carlsson, C.J.H. Jacobsen, Chem. Mater., 13 (2001) 4416-4418.

[10] L. Tosheva, J. Sterte, ZSM-5 spheres prepared by resin templating, in: R. Aiello, G. Giordano, F. Testa (Eds.) Impact of Zeolites and Other Porous Materials on the New Technologies at the Beginning of the New Millennium, Pts a and B, 2002, pp. 183-190.

[11] M. Choi, H.S. Cho, R. Srivastava, C. Venkatesan, D.H. Choi, R. Ryoo, Nat. Mater., 5 (2006) 718-723.

[12] M. Choi, R. Srivastava, R. Ryoo, Chem. Comm., (2006) 4380-4382.

[13] Y. Wan, D.Y. Zhao, Chem. Rev., 107 (2007) 2821-2860.

[14] J.C. Groen, J.C. Jansen, J.A. Moulijn, J. Perez-Ramirez, J. Phys. Chem. B, 108 (2004) 13062-13065.

[15] J.C. Groen, L.A.A. Peffer, J.A. Moulijn, J. Perez-Ramirez, Microporous and Mesoporous Mater., 69 (2004) 29-34.

[16] J.C. Groen, L. Maldonado, E. Berrier, A. Brückner, J.A. Moulijn, J. Pérez-Ramírez, J. Phys. Chem. B, 110 (2006) 20369-20378.

[17] J.C. Groen, J.A. Moulijn, J. Perez-Ramirez, J. Mater. Chem., 16 (2006) 2121-2131.

[18] D. Verboekend, S. Mitchell, M. Milina, J.C. Groen, J. Perez-Ramirez, J. Phys.Chem. C, 115 (2011) 14193-14203.

[19] D. Verboekend, J. Perez-Ramirez, Chem. Europ. J., 17 (2011) 1137-1147.

[20] D. Verboekend, J. Perez-Ramirez, Catal. Sci. & Technol., 1 (2011) 879-890.

[21] T. Martin, A. Galarneau, F.D. Renzo, F. Fajula, D. Plee, Angew. Chem.-Int. Edit., 41 (2002) 2590-2592.

[22] S.B. Yoon, J.-Y. Kim, J.H. Kim, Y.J. Park, K.R. Yoon, S.-K. Park, J.-S. Yu, J. Mater. Chem., 17 (2007) 1758-1761.

[23] S. Inagaki, M. Ogura, T. Inami, Y. Sasaki, E. Kikuchi, M. Matsukata,.Microporous and Mesoporous Mater., 74 (2004) 163-170.

[24] Y.D. Xia, R. Mokaya, J.Mater. Chem., 14 (2004) 863-870.

[25] C.E.A. Kirschhock, S.P.B. Kremer, J. Vermant, G. Van Tendeloo, P.A. Jacobs, J.A. Martens, Chem. Europ. J., 11 (2005) 4306-4313.

[26] Q. Tang, H. Xu, Y. Zheng, J. Wang, H. Li, J. Zhang, Appl. Catal. A, 413-414 (2012) 36-42.

[27] V.V. Ordomsky, V.Y. Murzin, Y.V. Monakhova, Y.V. Zubavichus, E.E. Knyazeva, N.S. Nesterenko, I.I. Ivanova, Microporous and Mesoporous Mater., 105 (2007) 101-110.

[28] J.Y. Ying, J. Garcia-Martinez, US Patent 2005/0239634 A1.

[29] J. Garcia-Martinez, US Patent 8,008,223 B2

[30] J. Garcia-Martinez, M. Johnson, J. Valla, K. Li, J.Y. Ying, Catal. Sci. & Technol., 2 (2012) 987-994.

[31] W.C. Yoo, X. Zhang, M. Tsapatsis, A. Stein, Microporous and Mesoporous Mater., 149 (2012) 147-157.

[32] P.A. Jacobs, J.A. Martens (Ed), Synthesis of High-Silica Aluminosilicate Zeolites, Stud. Surf. Sci. Catal., 33, (1987) 3-111.

[33] D. Verboekend, A.M. Chabaneix, K. Thomas, J.-P. Gilson, J. Perez-Ramirez, Cryst.Eng.Comm, 13 (2011) 3408-3416.

[34] M. S. Holm, S. Svelle, F. Joensen, P. Beato, C. H. Christensen, S. Bordiga, M. Bjørgen, Appl.Catal., A, 356 (2009) 23-30.

[35] S. M. Campbell, X.-Z. Jiang, R. F. Howe, , Microporous and Mesoporous Mater., 29 (1999) 91-108.

[36] D. Chen, H.P. Rebo, A. Holmen, Chem. Eng. Sci., 54 (1999) 3465-3473.

[37] J. Kim, M. Choi, R. Ryoo, J.Catal., 269 (2010) 219-228.

[38] I.M. Dahl, S. Kolboe, Catal. Lett., 20 (1993) 329-336.

[39] I.M. Dahl, S. Kolboe, J. Catal., 149 (1994) 458-464.

[40] M. Bjørgen, S. Svelle, F. Joensen, J. Nerlov, S. Kolboe, F. Bonino, L. Palumbo, S. Bordiga, U. Olsbye, J.Catal., 249 (2007) 195-207.

[41] J.F. Haw, W.G. Song, D.M. Marcus, J.B. Nicholas, Acc. Chem. Res., 36 (2003) 317-326.

[42] U. Olsbye, S. Svelle, M. Bjørgen, P. Beato, T.V.W. Janssens, F. Joensen, S. Bordiga, K.P. Lillerud, Angew. Chem., 124 (2012) 2-26.

[43] M. Bjørgen, F. Joensen, M.S. Holm, U. Olsbye, K.P. Lillerud, S. Svelle, Appl.Catal., A, 345 (2008) 43-50.

[44] C.S. Mei, P.Y. Wen, Z.C. Liu, H.X. Liu, Y.D. Wang, W.M. Yang, Z.K. Xie, W.M. Hua, Z. Gao, J. Catal., 258 (2008) 243-249.

[45] C. Liu, X. Wang, S. Lee, L.D. Pfefferle, G.L. Haller, Microporous and Mesoporous Mater., 147 (2012) 242-251.

Improved catalytic performance of hierarchical ZSM-5 synthesized by desilication with surfactants

Franz Schmidt[a], Martin R. Lohe[a,b], Bernd Büchner[b], Filippo Giordanino[c], Francesca Bonino[c], Stefan Kaskel[a,d]

[a] Department of Inorganic Chemistry, Dresden University of Technology, Bergstr. 66, 01069 Dresden, Germany

[b] Leibniz Institute for Solid State and Materials Research Dresden (IFW Dresden), Institute for Solid State Research, Helmholtzstrasse 20, 01069 Dresden, Germany

[c] Department of Chemistry, NIS Centre of Excellence, and INSTM Centro di Riferimento, University of Turin, Via P. Giuria 7, I-10125 and Via Quarello 11, I-10135, Torino, Italy.

[d] Fraunhofer Institute for Material and Beam Technology IWS, Winterbergstr. 28, 01277 Dresden, Germany

Supplementary Data

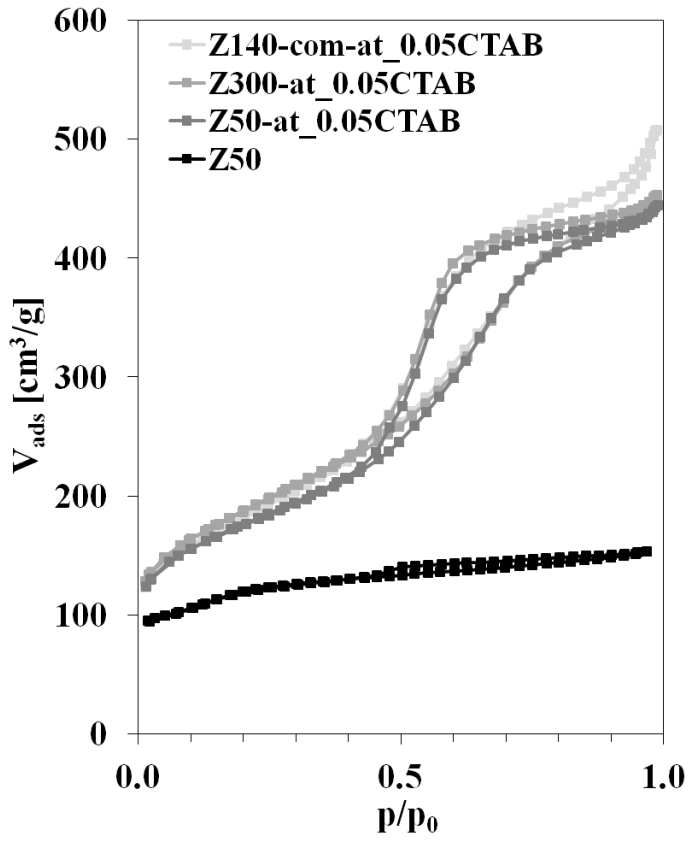

Figure S1: Nitrogen physisorption isotherms of the co-surfactant desilicated ZSM-5 material. Zeolites with a chemical composition of Si/Al = 50, 140 and 300 were used as starting materials. The zeolites with the composition Si/Al = 50 and 300 are synthesized in the laboratory and the zeolite with Si/Al = 140 is commercial. The isotherms clearly visualize that the desilication re-assembly process does not depend on the zeolite composition.

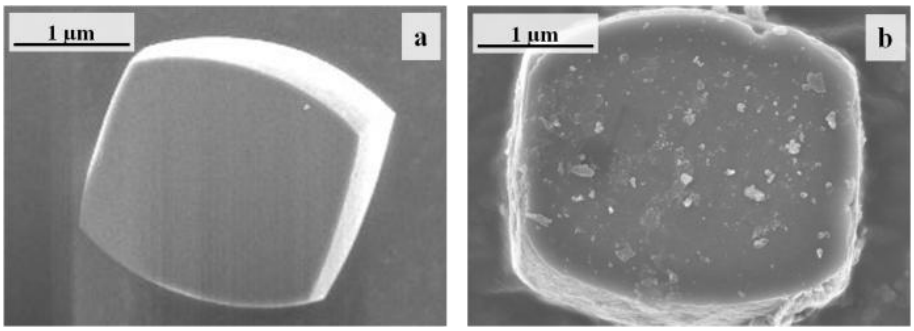

Figure S2: SEM pictures of the parent zeolite (Z300; Si/Al = 300) and the desilicated re-assembled zeolite (Z300-at_0.05CTAB). The morphology of the particle is remained.

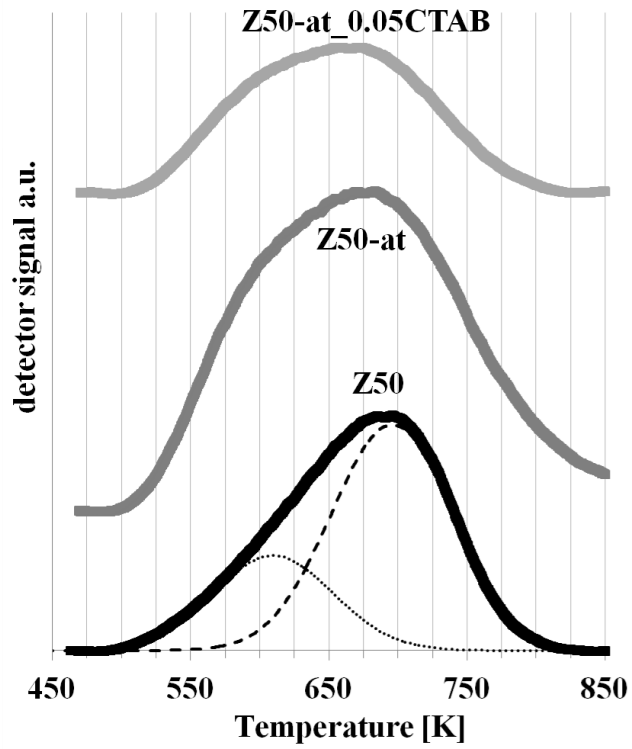

Figure S3: TPAD profiles of the parent zeolite (Z50), the desilicated (Z50-at) and the desilicated reassembled (Z50-at_0.05CTAB) material. Both desilicated samples show a distinctive shoulder at 550 – 650 K, resulting from different acid sites. To evaluate the strong acid sites two Gaussian peaks were fitted under each curve with the least square method [1].

Table S1: Acidic properties of the parent zeolite (Z50), the desilicated (Z50-at) and the desilicated reassembled (Z50-at_0.05CTAB) material.

	Si/Al [a]	NH_3 [b] capacity	v(OH)	Δv(OH)	v(CO)
	[mol mol^{-1}]	[mmol g^{-1}]	[cm^{-1}]	[cm^{-1}]	[cm^{-1}]
Z50	51	0.186	3614	336	2173
Z50-at	14	0.210	3617	331	2173
Z50-at_0.05CTAB	25	0.076	3612	330	2175
Z100	112	0.086	-	-	-

[a] chemical composition was determined by ICP-OES

[b] NH_3 capacity was determined by NH_3-TPAD (Integration of the deconvoluted strong acid site peak)

Chemical composition, the amount of desorbed ammonia (in the temperature range of 500 – 800 K, the vibrational mode of the Brönsted-acid sites (v(OH)), the shift upon CO adsorption and the vibrational mode of the CO molecules induced by Brönsted-acid sites.

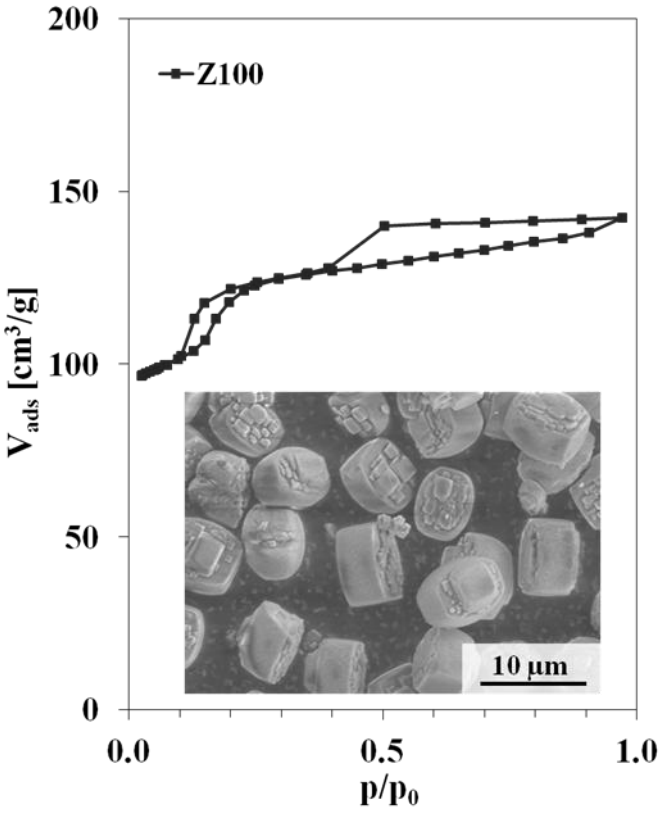

Figure S4: Nitrogen physisorption isotherms and SEM-picture of ZSM-5 (Z100) with similar acidic properties of the alkaline surfactant treated material (Z50-at_0.05CTAB). Besides the pure microporosity two hysteresis steps are visible which are subscribed to material effects. The hysteresis at p/p_0 = 0.2 is typical for ZSM-5 zeolites with Si/Al ratios above 75 and is caused by an expansion of the channels and an increased adsorption of nitrogen. The hysteresis at p/p_0 = 0.4 – 1 is assigned to interparticle voids.

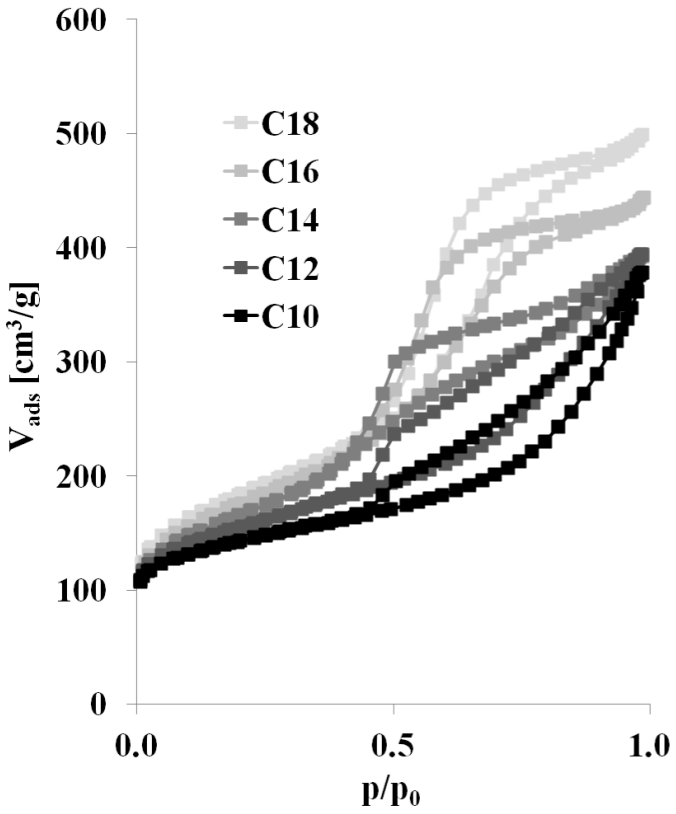

Figure S5: Nitrogen physisorption isotherms of the desilicated re-reassembled materials, using different surfactant molecules. The denotation C10 – C18 corresponds to the C atoms of the longest alkyl chain of the surfactant used. The development from the isotherm typical for purely desilication towards the typical isotherm of desilicated reassembled materials is clearly visible.

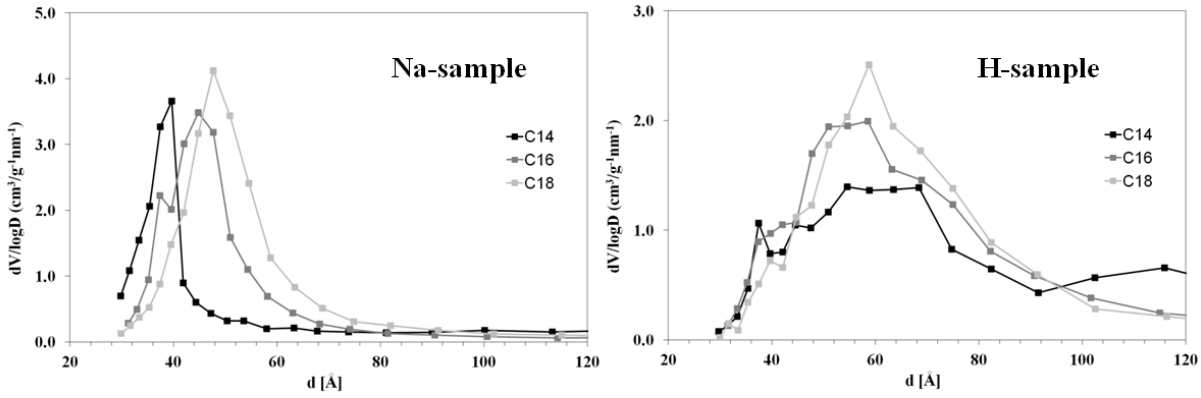

Figure S6: The pore size distribution of the samples co-templated with tetradecyltrimethylammonium bromide (C14), hexadecyltrimethylammonium bromide (C16) and octadecyltrimethylammonium bromide (C18) derived from the desorption branch of the nitrogen physisorption isotherm. Shown are the sodium and the ion-exchanged form of these samples. It is clearly visible, that the definite difference in pore size is destroyed upon ion exchange.

Literature

[1] J.C. Groen, J.A. Moulijn, J. Perez-Ramirez, Microporous and Mesoporous Mater., 87 (2005) 153-161.